Improving the accuracy of head rotation angle estimation using inertial micro-electro-mechanical sensors and adaptive digital filters

Ha Ngoc Khoan[1], Tran Van Nghia[2*], Le Ky Bien[1]

[1]Academy of Military Science and Technology, 17 Hoang Sam, Cau Giay, Hanoi, Vietnam;
[2]Air Force - Air Defense Technical Institute, 166 Hoang Van Thai, Thanh Xuan, Hanoi, Vietnam.
[*]Corresponding author: nghiamosmipt@gmail.com
Received 01 Jan. 2025; Revised 26 Mar. 2025; Accepted 10 Jun. 2025; Published 25 Jun. 2025.
DOI: https://doi.org/10.54939/1859-1043.j.mst.104.2025.59-70

ABSTRACT

The paper proposes a method to enhance the accuracy of head rotation angle estimation by integrating micro-inertial measurement sensors and digital filtering. The method is implemented under a stable gaze condition. Experimental results show that, compared to Mahony and Kalman filters, the proposed approach significantly improves the accuracy of head rotation angle estimation, with an RMS error of less than 0.1 degrees in horizontal plane rotation while maintaining real-time performance. These results are well-suited for applications in vestibulo-ocular reflex (VOR) signal recording for vestibular disorder diagnosis.

Keywords: Vestibulo-ocular reflex (VOR); Inertial measurement unit (IMU); Adaptive digital filtering; Mahony filter; Head angular velocity; Micro-electromechanical sensors (MEMS).

1. INTRODUCTION

The vestibulo-ocular reflex (VOR) is considered as an automatic control system, where the input is head movement and the output is eye movement, aiming to maintain visual stability and body balance during head motion [3, 4]. By providing input stimuli and recording output signals, it is possible to model and analyze the vestibular system to explain the causes of dizziness and imbalance disorders. Accurate detection and diagnosis of these disorders are of significant medical importance but remain challenging for clinical-support technical devices.

One of the methods for assessing vestibular function involves measuring head rotation and observing eye movements during vestibular reflex tests [6]. To achieve measurements closely aligned with true values, precise gyroscopes, such as ring laser gyroscopes, are overly expensive and bulky for most practical applications. Therefore, the use of advanced measurement devices such as inertial measurement units (IMUs) is becoming a trend [1]. Researchers have utilized compact, accurate, and affordable inertial measurement unit (IMU) sensors and developed algorithms to compute angular kinematics of one or more body segments in biomechanics and clinical applications [10-14]. IMUs can measure both rotational and linear head movements using micro-electro-mechanical sensors, including accelerometers, gyroscopes, and magnetometers [4]. However, signals from IMUs often contain accumulated errors and noise [5], negatively impacting measurement accuracy.

The Kalman filter [9, 15] has become a widely accepted basis for the most accurate and efficient orientation filtering algorithms. However, Kalman-based solutions require significant computational resources, posing a major challenge for deploying compact devices used in VOR examination. The Mahony filter [7] demonstrates high performance under dynamic conditions by using a PI feedback loop, enhancing stability and providing rapid response when estimating rotation angles from inertial micro-electro-mechanical sensors (IMU). It effectively suppresses noise from accelerometers and magnetometers, reducing drift and increasing accuracy compared to simpler filters. With its lightweight computational structure, the Mahony filter is particularly suitable for microcontrollers and real-time embedded systems. However, in environments with strong magnetic interference or high vibration, the filter's performance can be affected due to

sensor calibration processes being less optimal compared to advanced nonlinear methods.

In this paper, the authors propose combining an IMU with an adaptive digital filter to enhance the estimation of head rotational velocity. The proposed method calculates a single estimated orientation angle through an optimal fusion of measurements from gyroscopes, accelerometers, and magnetometers, ensuring real-time performance for vestibular reflex examination procedures. The novel aspects of the proposed adaptive filtering approach include: a gradient descent algorithm compatible with sensors from various manufacturers; an online magnetic distortion compensation algorithm; gyroscope drift bias compensation; and elimination of the effects caused by sensor placement relative to the center of rotation. The paper also evaluates and compares the performance of the proposed method against Mahony, Kalman, and conventional digital filters on the same dataset. Simulation results demonstrate that the proposed method significantly improves the accuracy of head rotation angle measurement, meeting the requirements for clinical vestibular diagnostic applications.

2. METHOD

The method for estimating the orientation angle of head rotation is illustrated in figure 1. The adaptive digital filtering algorithm is designed to estimate the relative orientation angle between the sensor coordinate system and the Earth coordinate system (figure 2a), based on measurement data from accelerometer, magnetometer, and gyroscope sensors. In this paper, the following notations are used: Subscripts S and E denote quantities in the sensor coordinate system (Sensor – S) and Earth coordinate system (Earth – E), respectively; the subscript S-E denotes relative quantities between coordinate system E and coordinate system S; the subscript *n* denotes discrete samples of quantities in the time domain. As shown in figure 2a, any rotational orientation of system S relative to system E can be achieved by a rotation through angle θ around the OA axis.

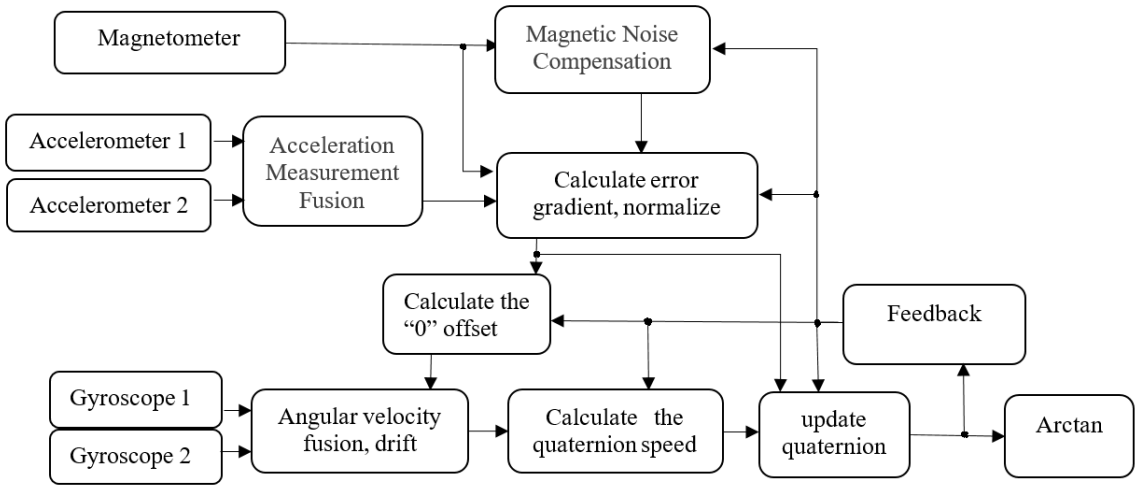

Figure 1. *Block diagram of the proposed adaptive digital filter for rotation angle measurement.*

A quaternion describing orientation does not impose restrictions on vector magnitude, so it is usually normalized. Thus, by convention, all orientation quaternions have unit length (1). The quaternion conjugate, denoted by $(.)^*$ can be used to switch between relative coordinate systems describing orientations. Therefore, $\hat{q}_{E-S}$ is the conjugate of $\hat{q}_{S-E}$ used to describe the relative orientation between the sensor coordinate system and the Earth coordinate system (2).

$$\hat{q}_{S-E} = \begin{bmatrix} q_1 & q_2 & q_3 & q_4 \end{bmatrix} = \begin{bmatrix} \cos\frac{\theta}{2} & -r_x \sin\frac{\theta}{2} & -r_y \sin\frac{\theta}{2} & -r_z \sin\frac{\theta}{2} \end{bmatrix} \quad (1)$$

$$\hat{q}^*_{S-E} = \hat{q}_{E-S} = \begin{bmatrix} q_1 & -q_2 & -q_3 & -q_4 \end{bmatrix} \quad (2)$$

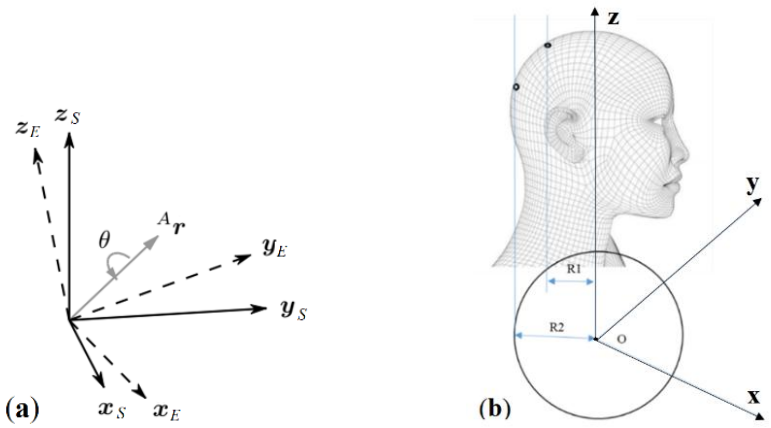

Figure 2. *Placement of two IMUs sensors.*

Suppose there is a system with two inertial measurement units (IMUs) attached to the head (figure 2b), rotating around the z-axis perpendicular to the horizontal plane. The two IMUs are oriented toward the center of rotation at distances of R_1 and $R_2 = R_1 + r$. The objective of the system (figure 1) is to determine the actual rotation angle of the head in the horizontal plane, which serves as the orientation parameter for eye movement at the moment of gaze stabilization, independent of sensor placement.

The three-degree-of-freedom (3-DOF) gyroscope measures angular velocity around the *x*, *y*, *z* axes within the sensor-fixed coordinate system, denoted as ω_x, ω_y, ω_z. Measurements from two gyroscopes ω_1 và ω_2 corresponding to equation (3), are input into the angular velocity fusion and drift compensation block (figure 1) to form a combined measurement signal as shown in equation (4). The angular velocity can be expressed in quaternion form, comprising components along the *x*, *y*, *z* axes in the sensor reference frame, as described by equation (5).

$$\omega_1 = \omega + c_1 + \eta_1, \qquad \omega_2 = \omega + c_2 + \eta_2 \tag{3}$$

$$\omega_S = \frac{1}{2}(\omega_1 + \omega_2) = \omega + \frac{1}{2}(c_1 + c_2) + \frac{1}{2}(\eta_1 + \eta_2) \tag{4}$$

$$\omega_S = \begin{bmatrix} 0 & \omega_x & \omega_y & \omega_z \end{bmatrix} \tag{5}$$

where ω is the actual rotational velocity of the head; c_1, c_2 represent the gyroscope drift (or zero offset), slowly varying over time; and η_1, η_2 denote measurement noise, assumed to be white noise.

Gyroscope drift varies over time, temperature, and motion, while measurement noise can be considered very small under conditions of low rotational velocity in VOR examination applications. Both gyroscope drift and measurement noise can be compensated by the proposed adaptive digital filter through integral feedback of orientation rate errors. Assuming that the normalized orientation estimation error $\dot{\hat{q}}_{e,S-E}$ and the actual estimated orientation $\hat{q}_{est}$ are obtained through the proposed filter, the angular measurement error ω_e for each gyroscope axis can be expressed in discrete form as shown in equation (6).

$$\omega_{e,S}(n) = 2\hat{q}^*_{est,S-E}(n-1) \otimes \dot{\hat{q}}_{e,S-E}(n) \tag{6}$$

where $\otimes$ denotes quaternion multiplication.

The gyroscope drift ω_b is represented by the DC component of ω_e and thus can be eliminated by integrating ω_e with a weighting coefficient ζ as shown in equation (7). The drift and the fused angular velocity measurement (5) are fed into the drift compensation block to generate drift-compensated gyroscope measurements (8), as illustrated in figure 1.

$$\omega_{b,S}(n) = \zeta \sum_{n} \omega_{e,S}(n) T \tag{7}$$

$$\omega_{c,S}(n) = \omega_S(n) - \omega_{b,S}(n) \tag{8}$$

where T is the sampling period.

The quaternion derivative representing the rate of change of orientation in the Earth coordinate system relative to the sensor coordinate system is expressed in equation (9). By numerically integrating this quaternion derivative, the orientation in the Earth coordinate system relative to the sensor coordinate system can be computed as shown in equation (10). Consequently, the estimated samples of actual orientation are simultaneously fed into both the quaternion rate estimation block and the quaternion integration update block (see figure 1). Another input to the quaternion rate estimation block is the drift-compensated gyroscope measurement $\omega_{c,S}$ used to compute the quaternion derivative, which then feeds into the remaining input of the quaternion integration update block.

$$\dot{q}_{\omega,S-E}(n) = \frac{1}{2} \hat{q}_{est,S-E}(n-1) \otimes \omega_{c,S}(n) \tag{9}$$

$$q_{\omega,S-E}(n) = \hat{q}_{est,S-E}(n-1) + \dot{q}_{\omega,S-E}(n) T \tag{10}$$

However, to directly utilize measurement (10) for determining the actual orientation of head rotation, the proposed filter needs to calculate the normalized orientation estimation error $\hat{\dot{q}}_{e,S-E}$. This quantity can be obtained by fusing measurements from accelerometer and magnetometer sensors.

The centripetal acceleration measurements from the two accelerometers $\hat{a}_1$, $\hat{a}_2$ (figure 1) are represented by equation (11). These acceleration measurements are sent to the acceleration fusion block to eliminate their dependence on the distance to the center of rotation through equation (12), and their quaternion representation is expressed in equation (13). It can be observed from equation (12) that the fused angular acceleration measurement is independent of the distance to the center of rotation and only depends on the relative distance *r* between the two IMU placements. This relative distance *r* is constant in the design of the VOR recording device.

$$\hat{a}_1 = R_1 \omega^2 + v_1, \qquad \hat{a}_2 = R_2 \omega^2 + v_2 \tag{11}$$

$$\hat{a}_S = \hat{a}_2 - \hat{a}_1 = r\omega^2 + (v_2 - v_1) \tag{12}$$

$$\hat{a}_S = \begin{bmatrix} 0 & a_x & a_y & a_z \end{bmatrix} \tag{13}$$

where v_1,v_2 are measurement noises from accelerometers, assumed to be white noise with small magnitudes due to slow changes in actual rotational speed (acceleration).

A three-axis accelerometer measures the magnitude and direction of the gravitational field in the sensor coordinate system, combined with linear acceleration due to sensor motion. Meanwhile, a three-axis magnetometer measures the magnitude and direction of the Earth's magnetic field in the sensor frame, incorporating local magnetic flux and distortion. However, measurements from these sensors contain noise and do not yield a unique sensor orientation solution; instead, there are infinite solutions representing all orientations achieved by rotating the true orientation around an axis parallel to the field, making direct use of these measurements unreliable. Therefore, a quaternion representation requires an optimal solution.

The quaternion representation of the reference orientation of the magnetic field in the Earth-fixed frame $\hat{d}_E$ and the measured orientation of the magnetic field in the sensor coordinate system $\hat{s}_S$ is defined through equations (14) and (15). The quaternion describing orientation (1) is the alignment that matches the direction of $\hat{d}_E$ with the measured direction $\hat{s}_S$. Therefore, $\hat{q}_{S-E}$ can

be determined as the solution that minimizes the objective function (16), (17).

$$\hat{d}_E = \begin{bmatrix} 0 & d_x & d_y & d_z \end{bmatrix} \tag{14}$$

$$\hat{s}_S = \begin{bmatrix} 0 & s_x & s_y & s_z \end{bmatrix} \tag{15}$$

$$\min_{\hat{q}_{S-E}} f\left(\hat{q}_{S-E}, \hat{d}_E, \hat{s}_S\right) \tag{16}$$

$$f\left(\hat{q}_{S-E}, \hat{d}_E, \hat{s}_S\right) = \hat{q}^*_{S-E} \otimes \hat{d} \otimes \hat{q}_{S-E} - \hat{s}_S \tag{17}$$

Before determining the optimal solution (16), it can be assumed that the direction of gravity is defined solely along the vertical *z*-axis. To establish the rotational orientation, the measured gravity from the sensor can be normalized as expressed in equation (18).

$$\hat{g}_E = \begin{bmatrix} 0 & 0 & 0 & 1 \end{bmatrix} \tag{18}$$

Substituting equations (13), (14), (15), and (18) into (17) yields the gravity-based objective function (19) and the Jacobian representation of the objective function (20) below.

$$f_g\left(\hat{q}_{S-E}, \hat{a}_S\right) = \begin{bmatrix} 2\left(q_2 q_4 - q_1 q_3\right) - a_x \\ 2\left(q_1 q_2 - q_3 q_4\right) - a_y \\ 1 - q_2^2 - q_3^2 - a_z \end{bmatrix} \tag{19}$$

$$J_g\left(\hat{q}_{S-E}\right) = \begin{bmatrix} -2q_3 & 2q_4 & -2q_1 & 2q_2 \\ 2q_2 & 2q_1 & 2q_4 & 2q_3 \\ 0 & -4q_2 & -4q_3 & 0 \end{bmatrix} \tag{20}$$

The Earth's magnetic field can be considered to have components along a horizontal *x*-axis and a vertical *z*-axis. Therefore, the magnetic field in the Earth-fixed reference frame $\hat{b}_E$ can be represented by equation (21), while the magnetometer measurements in the sensor coordinate system $\hat{m}_S$ include full components along three axes (22).

$$\hat{b}_E = \begin{bmatrix} 0 & b_x & 0 & b_z \end{bmatrix} \tag{21}$$

$$\hat{m}_S = \begin{bmatrix} 0 & m_x & m_y & m_z \end{bmatrix} \tag{22}$$

Substituting equations (14), (15), (21), and (22) into (17) yields the magnetic field-based objective function (23) and the Jacobian representation of this objective function (24) below.

$$f_b\left(\hat{q}_{S-E}, \hat{b}_E, \hat{m}_S\right) = \begin{bmatrix} 2b_x\left(0.5 - q_3^2 - q_4^2\right) + 2b_z\left(q_2 q_4 - q_1 q_3\right) - m_x \\ 2b_x\left(q_2 q_3 - q_1 q_4\right) + 2b_z\left(q_1 q_2 + q_3 q_4\right) - m_y \\ 2b_x\left(q_1 q_3 + q_2 q_4\right) + 2b_z\left(0.5 - q_2^2 - q_3^2\right) - m_z \end{bmatrix} \tag{23}$$

$$J_b\left(\hat{q}_{S-E}, \hat{b}_E\right) = \begin{bmatrix} -2b_z q_3 & 2b_z q_4 & -4b_x q_3 - 2b_z q_1 & -4b_x q_4 + 2b_z q_2 \\ -2b_x q_4 + 2b_z q_2 & 2b_x q_3 + 2b_z q_1 & 2b_x q_2 + 2b_z q_4 & -2b_x q_1 + 2b_z q_3 \\ 2b_x q_3 & 2b_x q_4 - 4b_z q_2 & 2b_x q_1 - 4b_z q_3 & 2b_x q_2 \end{bmatrix} \tag{24}$$

As analyzed above, individual measurements of Earth's gravity or magnetic field alone do not provide a unique orientation for the sensor. To obtain a unique orientation solution, the measurements and reference directions of both fields can be combined as described by expressions (25) and (26), where the superscript *T* denotes the transpose operation.

$$f_{g,b}\left(\hat{q}_{S-E},\hat{a}_S,\hat{b}_E,\hat{m}_S\right)=\begin{bmatrix} f_g\left(\hat{q}_{S-E},\hat{a}_S\right) \\ f_b\left(\hat{q}_{S-E},\hat{b}_E,\hat{m}_S\right)\end{bmatrix} \tag{25}$$

$$J_{g,b}\left(\hat{q}_{S-E},\hat{b}_E\right)=\begin{bmatrix} J_g^T\left(\hat{q}_{S-E}\right) \\ J_b^T\left(\hat{q}_{S-E},\hat{b}_E\right)\end{bmatrix} \tag{26}$$

To achieve the solution that minimizes the objective function, the proposed adaptive algorithm employs the gradient descent method due to its simplicity in implementation and computation among existing optimization algorithms. To enhance convergence efficiency, the proposed adaptive algorithm adjusts the step size μ to an optimal value at each iteration. The gradient descent algorithm's estimated orientation angle is calculated via equation (27). The gradient of the objective function ∇f is determined by accelerometer $\hat{a}_S(n)$ and magnetometer $\hat{m}_S(n)$ sensor measurements sampled at time *n* as shown in equation (28).

$$q_{\nabla,S-E}(n)=\hat{q}_{est,S-E}(n-1)-\mu(n)\frac{\nabla f}{\|\nabla f\|} \tag{27}$$

$$\nabla f=J_{g,b}^T\left(\hat{q}_{est,S-E}(n-1),\hat{b}_E\right)f_{g,b}\left(\hat{q}_{est,S-E}(n-1),\hat{a}_S(n),\hat{b}_E(n),\hat{m}_S(n)\right) \tag{28}$$

where the subscript ∇ indicates that the quaternion is computed using the gradient descent algorithm; the optimal value $\mu(n)$ is defined as the value ensuring the convergence rate of $q_{\nabla,S-E}(n)$ bounded by the physical orientation rate to avoid overcorrection if the step size is too large. The value $\mu(n)$ at each iteration is calculated according to equation (29).

$$\mu(n)=\alpha\left\|\dot{q}_{\omega,S-E}(n)\right\|T,\quad \alpha>1 \tag{29}$$

where $\dot{q}_{\omega,S-E}(n)$ is the physical orientation rate measured by the gyroscope, and α is the increment of μ to account for noise in accelerometer and magnetometer measurements.

The estimated orientation angle of the sensor coordinate system relative to the Earth-fixed reference frame $q_{est,S-E}(n)$ is derived from the quantities $q_{\omega,S-E}(n)$(10) and $q_{\nabla,S-E}(n)$(27) through equation (30).

$$q_{est,S-E}(n)=\gamma(n)q_{\nabla,S-E}(n)+\left(1-\gamma(n)\right)q_{\omega,S-E}(n),\quad 0\le\gamma(n)\le 1 \tag{30}$$

The filter parameter $\gamma(n)$ is used to ensure uniform convergence of $q_{\omega,S-E}(n)$ and $q_{\nabla,S-E}(n)$ and is calculated by equation (31), where $\frac{\mu(n)}{T}$ and $\beta(n)$ is the corresponding convergence rate of $q_{\omega,S-E}(n)$ and $q_{\nabla,S-E}(n)$.

$$\gamma(n)=\frac{\beta}{\frac{\mu(n)}{T}+\beta} \tag{31}$$

For the adaptive filter to achieve a fast convergence rate, the quantity $q_{\nabla,S-E}$ adjusted by α must converge faster than the device's physical orientation change rate. Therefore, α has no upper bound. If α is assumed to be very large, causing $\mu(n)$ to grow significantly, the quantities computed by the filter below are simplified as follows:

$$q_{\nabla,S-E}(n) \approx -\mu(n)\frac{\nabla f}{\|\nabla f\|};\ \gamma(n) \approx \frac{\beta T}{\mu(n)} \approx 0 \tag{32}$$

Therefore:

$$q_{est,S-E}(n) = \hat{q}_{est,S-E}(n-1) + \dot{q}_{est,S-E}(n)T \tag{33}$$

$$\dot{q}_{est,S-E}(n) = \dot{q}_{\omega,S-E}(n) - \beta\dot{\hat{q}}_{e,S-E}(n) \tag{34}$$

$$\dot{\hat{q}}_{e,S-E}(n) = \frac{\nabla f}{\|\nabla f\|} \tag{35}$$

The estimated true rotational orientation angle of the device (33) is required to accurately calibrate Earth's magnetic field measurements (21) due to measurement noise caused by the presence of ferromagnetic components, electrical devices, or metallic materials near the magnetometer. Magnetic field measurement errors can be compensated by the accelerometer, which provides supplementary measurements of the sensor's state. The measured direction of the Earth's magnetic field in the Earth-fixed reference frame $\hat{h}_E(n)$ is calculated from the normalized magnetometer measurement $\hat{m}_S(n)$, rotated by an angle relative to the sensor $\hat{q}_{est,S-E}(n-1)$ based on the filter's estimate, as described in equation (36).

$$\hat{h}_E(n) = \begin{bmatrix} 0 & h_x & h_y & h_z \end{bmatrix} = \hat{q}_{est,S-E}(n-1) \otimes \hat{m}_S(n) \otimes \hat{q}^*_{est,S-E}(n-1) \tag{36}$$

According to equation (21), the filter's reference direction for the Earth's magnetic field eliminates noise by computing $\hat{b}_E(n)$ similar to $\hat{h}_E(n)$, normalized to retain only the *x*- and *z*-axis components in the Earth-fixed reference frame (37).

$$\hat{b}_E(n) = \begin{bmatrix} 0 & \sqrt{h_x^2 + h_y^2} & 0 & h_z \end{bmatrix} \tag{37}$$

From equations (7) and (34), the filter gain β must be chosen such that all mean measurement errors of the gyroscope are zero, while the filter gain ζ represents the convergence rate to eliminate gyroscope measurement errors. For convenience, β and ζ can be expressed using the angular velocity $\tilde{\omega}_\beta$ and the rate of change of angular velocity $\dot{\tilde{\omega}}_\zeta$ where $\tilde{\omega}_\beta$ denotes the estimated zero-mean gyroscope measurement error per axis, and $\dot{\tilde{\omega}}_\zeta$ represents the estimated gyroscope bias drift rate per axis. Using equation (9), β and ζ can be calculated via equations (38) and (39).

$$\beta = \left\| \frac{1}{2}\hat{q} \otimes \begin{bmatrix} 0 & \tilde{\omega}_\beta & \tilde{\omega}_\beta & \tilde{\omega}_\beta \end{bmatrix} \right\| = \sqrt{\frac{3}{4}}\tilde{\omega}_\beta \tag{38}$$

$$\zeta = \left\| \frac{1}{2}\hat{q} \otimes \begin{bmatrix} 0 & \dot{\tilde{\omega}}_\zeta & \dot{\tilde{\omega}}_\zeta & \dot{\tilde{\omega}}_\zeta \end{bmatrix} \right\| = \sqrt{\frac{3}{4}}\dot{\tilde{\omega}}_\zeta \tag{39}$$

With the estimated quaternion (33) describing the orientation, three angular quantities ε, ψ, and ϕ rotating around the *z, y*, and *x* axes, respectively, in the Earth-fixed reference frame can be extracted. However, in VOR experiments, only the horizontal rotation angle ε of the head is of interest. Therefore, from equations (1) and (33), the angular quantity ε is computed using equation (40). This expression is not part of the proposed filter but is simply an Arctan function computation block, as illustrated in figure 1.

$$\varepsilon = \arctan 2\left(2q_2q_3 - 2q_1q_4, 2q_1^2 + 2q_2^2 - 1\right) \tag{40}$$

Through the above analysis, the proposed method and its operation based on the block diagram in figure 1 are described by algorithm 1, where the filter inputs are the measured quantities from the sensors, the filter output is derived from the quaternion update block, and the estimated head rotation angle is the output of the Arctan block.

Algorithm 1. Head Rotation Angle Estimation Based on Adaptive Filter

1. Use equation (4) to compute the fused angular velocity measurement from two gyroscopes;
2. Use equation (8) to combine the output of the zero-bias computation block and the fused angular velocity measurement, generating a drift-compensated angular rate at the output of the angular rate fusion and drift compensation block;
3. Calculate the quaternion rate using equation (9), which takes the product of the drift-compensated angular rate and the filter output;
4. Amplify the normalized error gradient; combine it with the quaternion rate computation block output in the quaternion update block through equations (34) and (33) to form the filter output;
5. Use magnetometer measurements and the filter output to cancel magnetic field noise via equations (36) and (37);
6. Use equation (12) to fuse centripetal acceleration measurements from two accelerometers;
7. Compute the error function gradient via equation (28), then normalize the gradient;
8. Calculate the head rotation angle using the Arctan function (40).

3. RESULTS AND DISCUSSION

Based on the characteristics of three specific stimuli designed to generate vestibular-ocular reflex (VOR) measurement signals in real-world applications, the following experiments evaluate the performance of the proposed adaptive digital filter in processing sensor data and compare it with another filter under three cases: Case1: **Sinusoidal horizontal head oscillation**; Case2: **Horizontal head oscillation followed by a stop**; Case3: **Arbitrary horizontal head oscillation** (see figure 3).

The experimental and comparative results are presented in figures 4–6 and table 1. For evaluation, the authors used MPU9250 sensors and an ATMEGA328P-AU microprocessor mounted on an Arduino R3 board to record signals and Basys 3 Artix-7 FPGA Digilent Board, followed by simulations conducted in MATLAB 2021a.

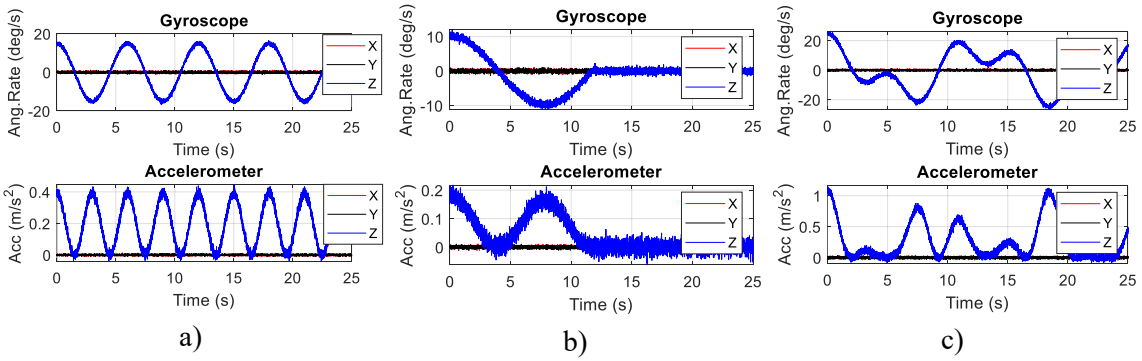

Figure 3. Data with measured sensor noise: a) Case1; b) Case2; c) Case3.

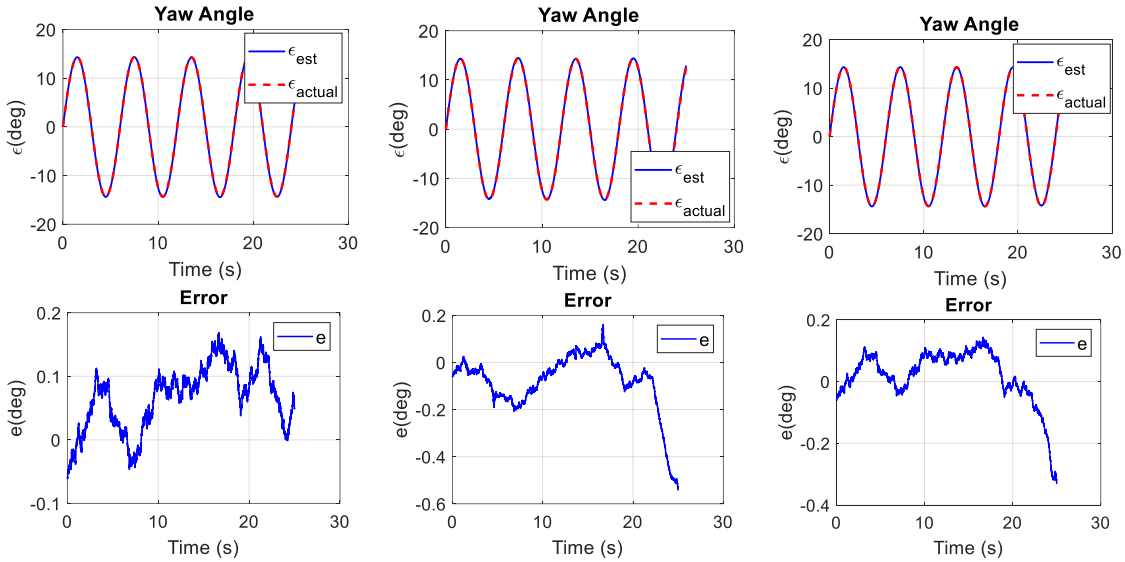

Figure 4. *Processing measurement data in Case1:*
a – Adaptive digital filtering; b – Mahony; c – Kalman.

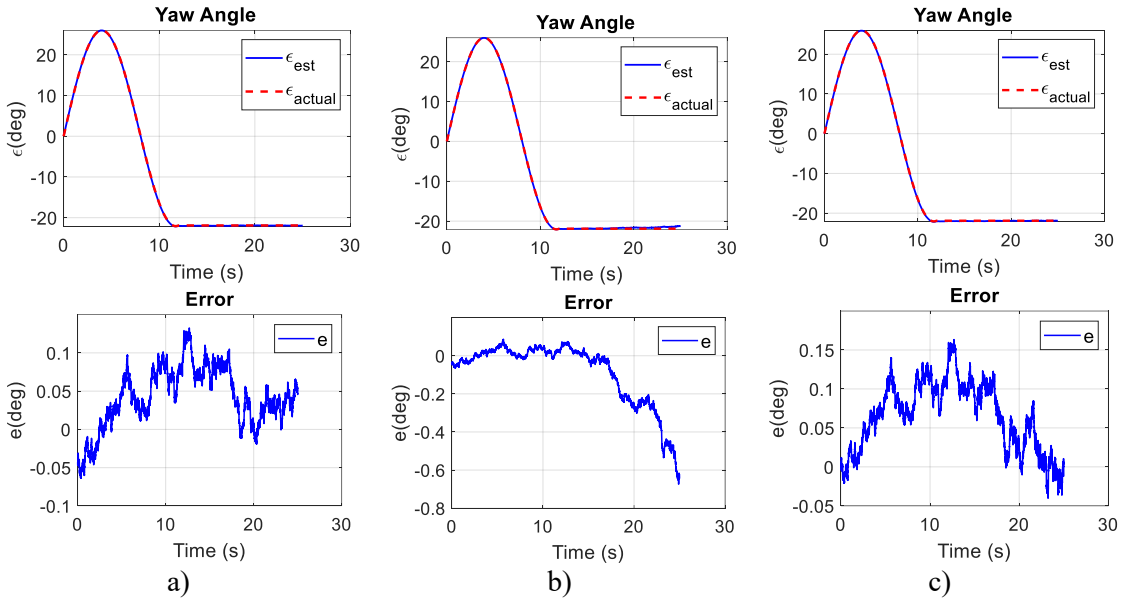

Figure 5. *Processing measurement data in Case2:*
a – Adaptive digital filtering; b – Mahony; c – Kalman.

Table 1. *Sensor Data Processing Comparison Results.*

Filter	RMSE, ^{0}		
	Case1	Case2	Case3
Adaptive digital filtering	0.0832	0.0577	0.0636
Mahony	0.1501	0.1876	0.2019
Kalman	0.1020	0.0788	0.2454

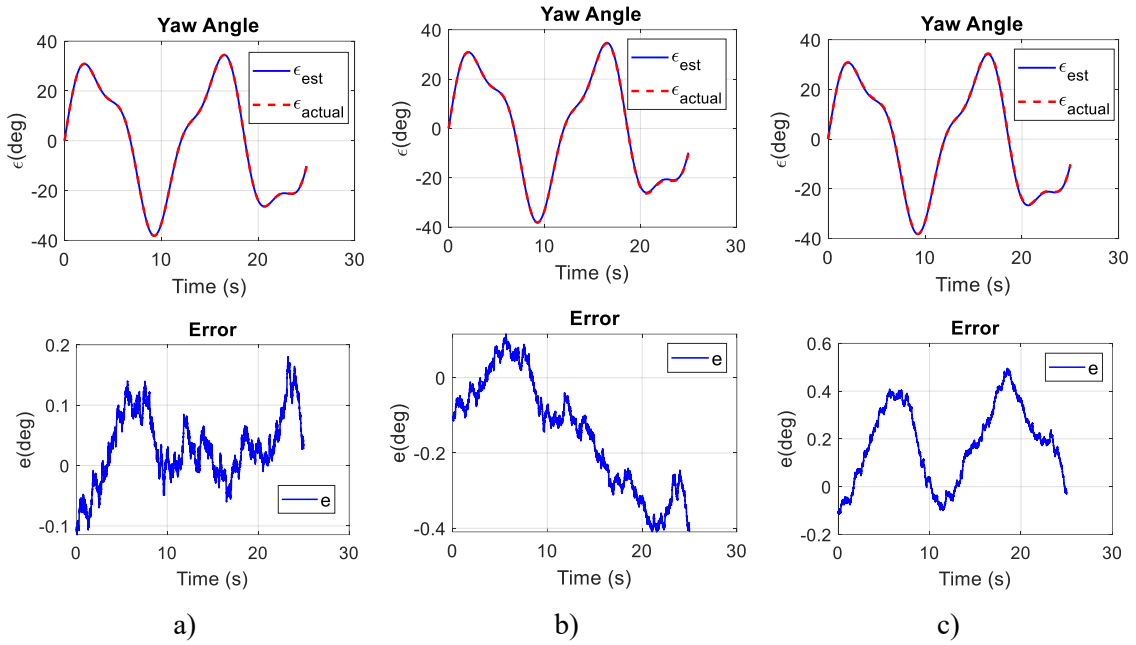

Figure 6. *Processing measurement data in Case3:*
a – Adaptive digital filtering; b – Mahony; c – Kalman.

From figures 3–6 and table 1, it can be observed that the proposed adaptive digital filter, the Mahony filter, and the Kalman filter provide head rotation angle estimates with small errors. However, the proposed adaptive digital filter ensures the smallest angular deviation compared to conventional Mahony and Kalman filters. The analysis also demonstrates that the proposed filter performs real-time magnetic distortion compensation and zero-bias drift correction for the gyroscope, further enhancing the accuracy of the estimated head rotation angle.

In practice, patients have different head sizes, and manufacturers design varying sensor placements for examination devices. Additionally, the position of the wearable device during each examination cannot be identical, which affects diagnostic results. A novel aspect of the proposed method, compared to existing approaches, lies in the use of paired gyroscopes and accelerometers to eliminate the influence of the relative sensor positions relative to the head's rotation center. The results in figures 7 and 8 illustrate tests conducted with different sensor placements but the same horizontal head rotation signal as in figure 3.

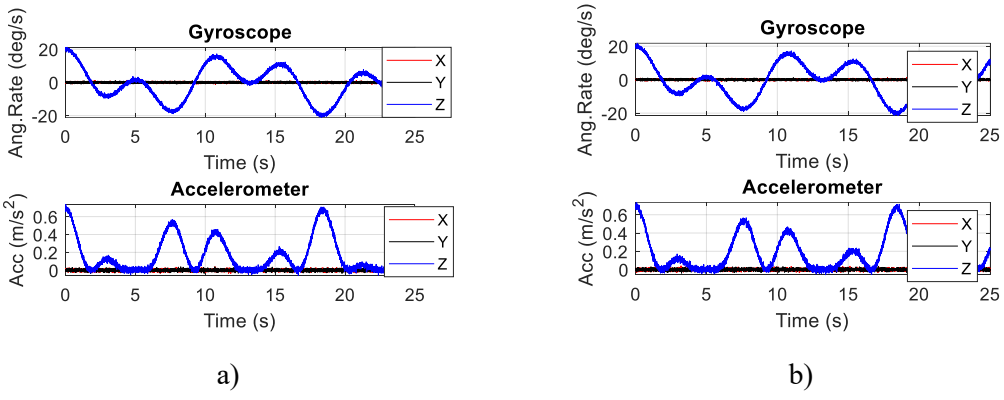

Figure 7. *Measurement data: a) R_1 = 5 cm; b) R_1 = 10 cm.*

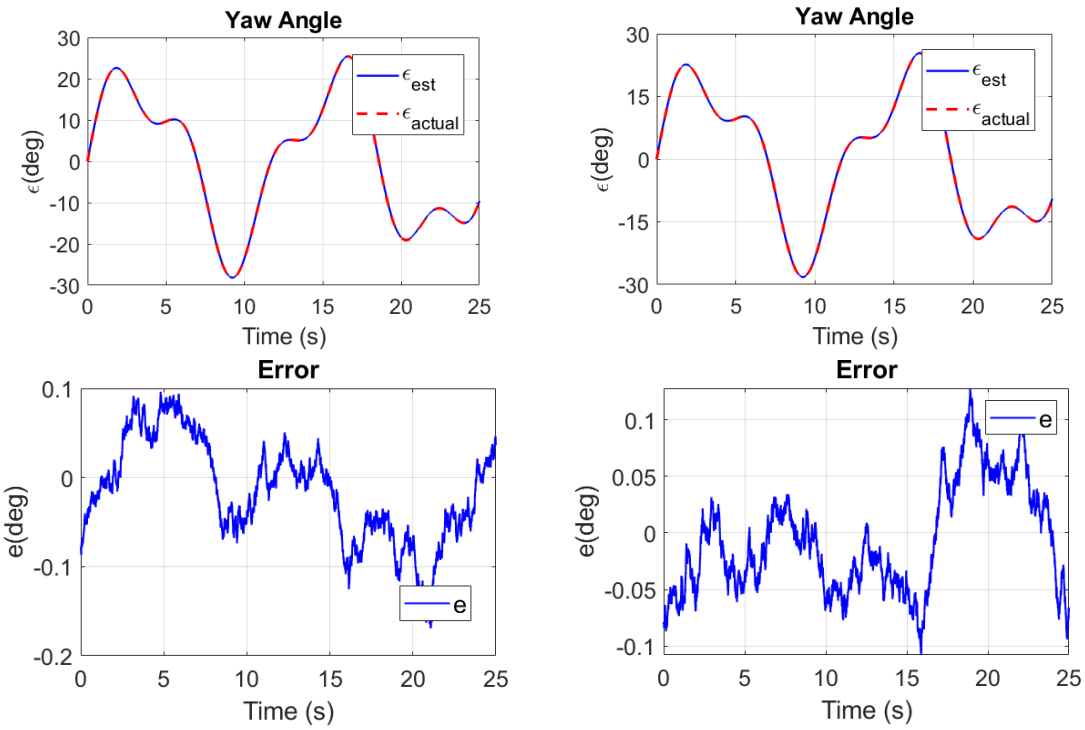

a) (RMSE = 0.0587) b) (RMSE = 0.0532)

Figure 8. *Measurement data using adaptive digital filter: a) R_1 = 5 cm; b) R_1 = 10 cm.*

From figures 7 and 8, it can be seen that the processing of the measured rotation angle for the same signal is not affected by the distance of the sensor placement on the head relative to the rotation center. This confirms that the proposed method for measuring head rotation angle in this study eliminates errors caused by sensor positioning deviations compared to currently used diagnostic devices.

4. CONCLUSIONS

This study applies an adaptive digital filter to integrate data from a MEMS gyroscope (with inherent drift) and a centripetal accelerometer (with measurement noise), enabling precise determination of head rotation angle and eye movement orientation parameters for the vestibular-ocular reflex (VOR) examination. The proposed solution, which employs two inertial measurement units (IMUs), eliminates the influence of sensor placement distance and position relative to the rotation axis (i.e., the radius from the sensor location to the rotation axis in the plane perpendicular to the rotation axis). This demonstrates the system's stability and reliability in real-world applications. The proposed method not only provides rapid computation suitable for real-time applications, such as measuring head rotation speed and angle, but also minimizes cumulative errors caused by noise and drift. This plays a critical role in delivering reliable input data for evaluating vestibular-ocular reflex signals during clinical VOR testing.

REFERENCES

[1]. V. Bijalwan, V. B. Semwal, T. K. Mandal. *"Fusion of Multi-Sensor Based Biomechanical Gait Analysis Using Vision and Wearable Sensor"*. IEEE Sensors Journal, vol. 21, no. 13, pp. 14213 - 14220, (2021).

[2]. S. O. Madgwick. *"An efficient orientation filter for inertial and inertial/magnetic sensor arrays"*. Report x-io and University of Bristol (UK), pp. 113-118, (2010).

[3]. S. Song, Y. Pei, & E. Hsiao-Wecksler. *"Estimating Relative Angles Using Two Inertial Measurement Units Without Magnetometers".* IEEE Sensors Journal, 22, 19688-19699, (2022).
[4]. S. A. Ludwig, & K. D. Burnham. *"Comparison of Euler Estimate using Extended Kalman Filter, Madgwick and Mahony on Quadcopter Flight Data".* International Conference on Unmanned Aircraft Systems (ICUAS), pp. 1236-1240, (2018).
[5]. A. Jouybari, H. Amiri, A. Ardalan, & N. Zahraee. *"Methods comparison for attitude determination of a lightweight buoy by raw data of IMU".* Measurement, 136, 490-500, (2019).
[6]. R.S. Jampel and D.C. Shi, *"Primary position of the eye, reset speed, and horizontal visual head plane. Head movements around the cervical joint"*, Investigative Ophthalmology & Visual Sciences 33, 2501–2510, (1992).
[7]. Mahony, R., Hamel, T., & Pflimlin, J. M. *"Nonlinear complementary filters on the special orthogonal group"*. IEEE Transactions on Automatic Control, 53(5), 1203–1218, (2008).
[8]. R. Kumar, M. Bhargavapuri, A. M. Deshpande, S. Sridhar, K. Cohen, and M. Kumar, *"Quaternion feedback based autonomous control of a quadcopter UAV with thrust vectoring rotors,"* 2020 American Control Conference (ACC), Denver, CO, USA, pp. 1-6, (2020). DOI: 10.23919/ACC45564.2020.9147794. https://ieeexplore.ieee.org/document/9147794
[9]. Q. Li, R. Li, K. Ji and W. Dai, *"Kalman Filter and Its Application,"* 2015 8th International Conference on Intelligent Networks and Intelligent Systems (ICINIS), Tianjin, China, pp. 74-77, (2015), doi: 10.1109/ICINIS.2015.35.
[10]. T. Seel, J. Raisch and T. Schauer, *"IMU-based joint angle measurement for gait analysis"*, *Sensors*, vol. 14, no. 4, pp. 6891-6909, (2014).
[11]. A. Brennan, J. Zhang, K. Deluzio and Q. Li, *"Quantification of inertial sensor-based 3D joint angle measurement accuracy using an instrumented gimbal"*, Gait Posture, vol. 34, no. 3, pp. 320-323, (2011).
[12]. S. Y. Song, Y. Pei, S. R. Tippett, D. Lamichhane, C. M. Zallek and E. T. Hsiao-Wecksler, *"Validation of a wearable position velocity and resistance meter for assessing spasticity and rigidity"*, Proc. Frontiers Biomed. Devices, pp. 1-4, (2018).
[13]. P. Picerno, *"25 years of lower limb joint kinematics by using inertial and magnetic sensors: A review of methodological approaches"*, Gait Posture, vol. 51, pp. 239-246, (2017).
[14]. S. Y. Song, Y. Pei, J. Liang and E. T. Hsiao-Wecksler, *"Design of a portable position velocity and resistance meter (PVRM) for convenient clinical evaluation of spasticity or rigidity"*, Proc. Design Med. Devices Conf., pp. 1-2, (2017).
[15]. G. Ligorio and A. M. Sabatini, *"A novel Kalman filter for human motion tracking with an inertial-based dynamic inclinometer"*, IEEE Trans. Biomed. Eng., vol. 62, no. 8, pp. 2033-2043, (2015).

TÓM TẮT

Nâng cao độ chính xác ước lượng góc quay của đầu sử dụng phần tử đo vi cơ quán tính và bộ lọc số thích nghi

Bài báo đề xuất phương pháp nâng cao độ chính xác ước lượng góc quay của đầu bằng cách kết hợp các cảm biến vi cơ quán tính và bộ lọc số. Phương pháp được triển khai trong trạng thái mắt ổn định ánh nhìn. Kết quả thử nghiệm cho thấy, so với bộ lọc Mahony, Kalman, giải pháp đề xuất cải thiện đáng kể độ chính xác ước lượng góc quay của đầu với lượng sai số RMS nhỏ hơn 0,1 độ theo góc quay trên mặt phẳng nằm ngang, đồng thời giữ được đặc tính thời gian thực. Kết quả này phù hợp với các ứng dụng của nghiên cứu ghi nhận tín hiệu phản xạ tiền đình - mắt trong chẩn đoán bệnh tiền đình.

Từ khoá: Phản xạ tiền đình-mắt (VOR); Đơn vị đo lường quán tính (IMU); Bộ lọc số thích nghi; Bộ lọc Mahony; Tốc độ quay của đầu; Cảm biến vi cơ (MEMS).